Background charge fluctuations and the transport properties of biopolymer-gold nanoparticle complexes

C. A. Berven,[a] M. N. Wybourne,[b] L. Clarke,[c] and L. Longstreth[d]
Department of Physics and Astronomy, Dartmouth College, Hanover, New Hampshire 03755

J. E. Hutchison and J. L. Mooster
Department of Chemistry, University of Oregon, Eugene, Oregon 97403

(Received 14 May 2002; accepted for publication 15 July 2002)

The room temperature electrical characteristics of biopolymer-gold nanoparticle complexes show threshold behavior, periodic conductance features, and current–voltage scaling that together indicate the nonlinear transport is associated with single electron charging. Repeated measurements over a period of up to 80 h showed the characteristics change with time. The current–voltage scaling behavior is found to be time independent, while the position of the conductance features shifted randomly over periods of many hours. We show that the time dependence is consistent with a fluctuating background charge distribution and can be understood within the framework of the orthodox model of single electron transport that is modified to account for the relatively large self-capacitance of the nanoparticles. © *2002 American Institute of Physics.*
[DOI: 10.1063/1.1506399]

I. INTRODUCTION

It has been recognized for sometime that metal particle systems exhibit highly nonlinear electron transport behavior related to single electron charging of the individual particles.[1–4] One signature of single electron behavior in chains of particles is a Coulomb staircase, the origin of which has been discussed by many people.[5–7] A Coulomb staircase is observed when the thermal energy is lower than the electrostatic charging energy that is determined by the effective capacitance of a particle.[8] The lower bound of the effective capacitance is set by the self-capacitance, which suggests that isolated spherical particles with radii on the nanometer scale will support single electron effects at room temperature. A Coulomb staircase also requires the tunneling resistance between particles to exceed the resistance quantum $h/2e^2$. This criterion is readily met by stabilizing metal particles with an organic ligand shell that isolates the particles and can provide a tunnel barrier between them.

Many synthesis routes have been developed to prepare semiconductor and metal particles with radii on the nanometer scale—nanoparticles.[9–14] Considerable progress has also been made toward the controlled assembly of one- and two-dimensional arrays of nanoparticles that are suitable for transport measurements.[15–19] Characterization of the perpendicular transport through two-dimensional arrays has shown evidence of single electron behavior at room temperature.[20–22] Lateral transport through two-dimensional arrays and one-dimensional chains created by templating techniques has also been shown to exhibit behavior associated with single electron charging.[23–26] Questions concerning the impact of structural and charge disorder, as well as the thermal, electrical and mechanical stability on the electrical characteristics are of particular importance for in-plane measurements.[27–29] Understanding these challenging issues will be essential for the development of any applications suggested by the nonlinear transport behavior of nanoparticle systems.[30,31]

In this article we discuss time dependent effects observed in the in-plane transport of ligand stabilized gold nanoparticles immobilized on the linear biopolymer poly-L-lysine. The room temperature transport through these disordered systems is found to have one-dimensional character and shows a well-defined, periodic Coulomb staircase. The position of the Coulomb staircase steps is observed to vary with time, reminiscent of the behavior reported to occur in traditional single electron devices when the background potential fluctuates due to charged two-level systems either inside or in the vicinity of the device.[32–36] We show that the extremely low frequency, dynamic current–voltage behavior of the present biopolymer-nanoparticle complexes can be explained by a fluctuating background charge distribution provided that the self-capacitance of the particles is accounted for in the calculation of tunneling rates (self-energy).

II. EXPERIMENT AND RESULTS

A wet chemical process was used to prepare nanoparticle networks on the polymer poly-L-lysine (PLL) between fingers of gold interdigitated array electrodes with gaps of 15 and 2 μm as described in detail elsewhere.[24] The average length of the PLL was determined from the molecular weight to be about 30 nm. Transmission electron microscopy micrographs of the nanoparticles showed a core radius of 0.7 $\pm$0.2 nm ($\pm$30%), with an estimated total radius including the ligand shell of 2.1 nm. PLL/nanoparticle assemblies were

[a]Present address: Department of Physics, University of Idaho, Moscow, ID 83844.
[b]Electronic mail: martin.n.wybourne@dartmouth.edu
[c]Present address: Department of Physics, University of Colorado at Boulder, Boulder, CO 80309.
[d]Present address: Berea College, Berea, KY 40404.

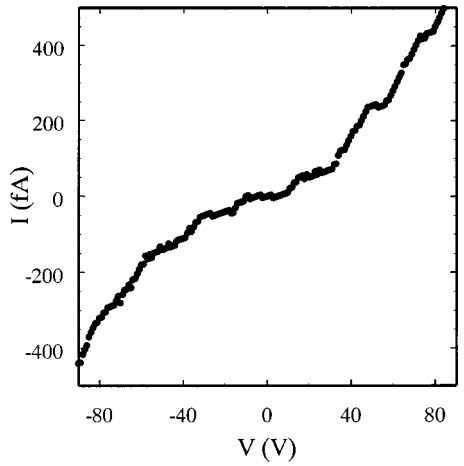

FIG. 1. The $I-V$ characteristics after decoration of the PLL with the gold nanoparticles and after the subtraction of the background conductance.

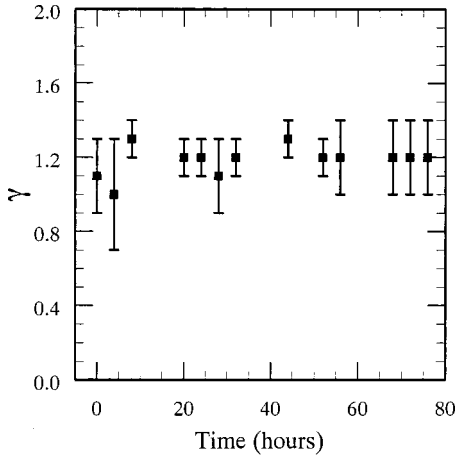

FIG. 2. The time evolution of the value of the $I-V$ scaling exponent γ. These data were obtained from a different sample to the one that gave the characteristic shown in Fig. 1.

also prepared on mica by the identical procedure. Atomic force microscopy (AFM) images of the mica-based samples showed that the method created a distribution of isolated quasi-one-dimensional structures of gold nanoparticles attached to the PLL biopolymer.[24] $I-V$ measurements were performed in an electrically shielded vacuum chamber as previously described.[19] Control measurements made on the bare electrodes and at several stages of fabrication before the introduction of the nanoparticles, showed a linear $I-V$ relationship that provides a typical background conductance of the apparatus and substrate $\sim 8\times 10^{-15}\ \Omega^{-1}$. After the PLL was decorated with nanoparticles, the $I-V$ characteristics became highly nonlinear with step-like features of about equal voltage spacing, which are seen clearly after the background conductance has been subtracted, as shown in Fig. 1. The data have an identifiable voltage threshold, $V_T \sim 12$ V, above which the current is nonzero and increases in a series of steps spaced by about 21 ± 4 V. At voltages well in excess of V_T the current scales as $I\propto(V/V_T-1)^{\gamma}$ with an average scaling exponent, $\gamma=1.2\pm 0.1$. Measurements of the $I-V$ behavior were carried out at different times up to 80 h from the start of the first measurement. Each measurement took about 1 h to complete. Using $V_T=12$ V for all sets of data, the scaling exponent was found to have no noticeable time dependence, as shown in Fig. 2. In contrast, the positions of the conductance peaks shift with time, as seen in Fig. 3, yet the periodicity and the magnitude of the peaks are relatively insensitive to time. The shift in the conductance peaks can be large enough that the voltage at which a conductance minimum occurs will, at some later time, correspond to a conductance maximum, as seen in Fig. 3, traces (b) and (c). This behavior suggests the presence of a fluctuating potential within the samples that varies on a time scale of many hours. We note that traditional single electron devices and the present PLL-nanoparticle complex devices reveal potential fluctuations differently: In the former case the periodicity of the Coulomb staircase is modulated, whereas in the latter case a ''phase shift'' is observed. We will show that this difference is associated with the ratio of the self-capacitance to the tunnel junction capacitance of the two systems.

III. DISCUSSION

The electronic degree of freedom in single-electron systems is known to be related to the value of scaling exponent γ.[37] An exponent close to unity is consistent with that predicted and measured in one-dimensional systems.[37–39] In contrast, for a two-dimensional system the experimental and theoretical value of the exponent is about two.[28,40] Thus, the measured value of $\gamma=1.2\pm 0.1$ for the PLL-nanoparticle complex suggests the transport is dominated by one-dimensional chains; the insensitivity of γ toward time shows that to within the measurement uncertainty the dimensionality characterizing the transport process is stable with time.

To understand the shifts of the conductance peaks with time we use the orthodox model[41,42] of single electron transport that we have extended to account for the dominant self-capacitance.[8] Initially, we consider an idealized chain of nanoparticles that has the equivalent circuit shown in Fig. 4. In a chain of nanoparticles there are three important capacitances: the capacitance between nanoparticles, C_i; the ca-

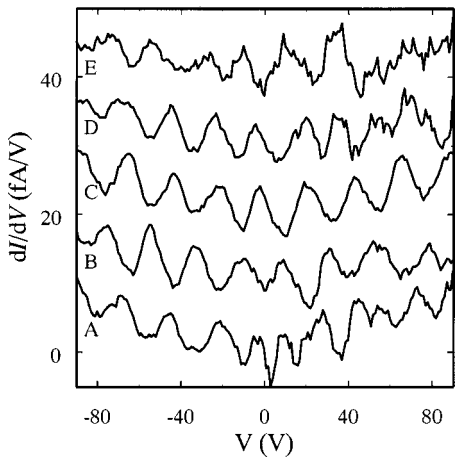

FIG. 3. Differential conductance plots taken at different times showing the time dependent nature of the $I-V$ structure. The plots have been offset by multiples of 10 fA/V for clarity. For each curve (a)–(e), the time at which the data was taken was 0 (a), 8 (b), 20 (c), 28 (d), and 52 h (e).

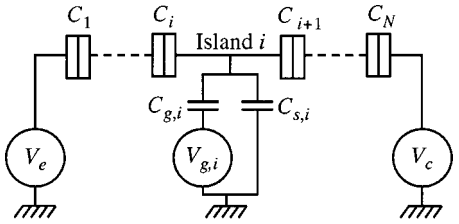

FIG. 4. Equivalent circuit of a chain of nanoparticles that includes the self-capacitance.

pacitance between each nanoparticle and a back-plane, $C_{g,i}$; and the self-capacitance of each nanoparticle, $C_{s,i}$, which is the capacitance to an infinitely distant ground plane. These capacitances have been calculated by treating the nanoparticles as 1.4 nm diameter metal cores surrounded by a 1.4-nm-thick dielectric shell of permitivity 3. The capacitance matrix calculated for a six nanoparticle chain gives a minimum interparticle capacitance $C_i \approx 0.04$ aF and a maximum self-capacitance $C_{s,i} \approx 0.17$ aF.[43] Thus, because of the nanoparticle size, the capacitance value $C_{s,i} > C_i$. Assuming the ligands do not interdigitate to any significant extent, the shell thickness sets a lower limit on the proximity of the metal cores. As a result, we expect $C_i \geqslant C_{g,i}$ so that the largest individual contribution to the total capacitance of a nanoparticle is $C_{s,i}$. The characteristic charging energy $E_c = e^2/2C_\Sigma \approx 0.3$ eV, where for each particle $C_\Sigma = C_{s,i} + 2C_i + C_{g,i}$, shows that the nanoparticles can support single electron charging effects at room temperature, just as observed. The value of E_c suggests that the conductance peaks should have a period of between about 0.6 and 0.9 V, whereas the observed period is about 20 V. Reducing C_Σ will increase the period. However, assuming the relationship between capacitance and the geometry of a particle remains valid at very small dimensions, the reduction in C_Σ necessary to explain the observed period would require unphysically small particles. AFM experiments show that the quasi-one-dimensional structures probably do not form a continuous path between the electrodes.[24] Therefore, the conduction path is expected to include regions between the quasi-one-dimensional structures. The conductance of these regions will be determined by the surface conduction of the substrate, which we have shown to be consistent with a thin water layer that results from the wet chemical fabrication method used to prepare the structures.[24] The surface conductance, together with contact resistance between the electrodes and the nanoparticle system, will introduce potential drops so that the voltage across the quasi-one-dimensional structures is only a fraction of the voltage applied to the sample. Since it is the voltage across the nanoparticle structure that is important for single electron behavior, the potential drops provide an explanation for the difference between the observed and predicted values of V_T. The nature of the current path has been addressed in more detail in Ref. 24.

The tunneling probability for an electron to tunnel from the particular island $k-1$ to k (Fig. 4), is well-known to be given by[41]

$$\Gamma_k(\mathbf{n}) = \frac{\Delta G_k(\mathbf{n})}{e^2 r_k (1 - \exp[-\Delta G_k(\mathbf{n})/k_B T])}, \tag{1}$$

where $\Delta G_k(\mathbf{n})$ is the difference in the free-energy of the system before and after the tunneling event has occurred and the initial electron occupancy on islands is given by $\mathbf{n} \equiv (n_1, n_2 \ldots n_{N-1})$. The tunneling resistance of tunnel-junction k is r_k and k_B and T are Boltzmann's constant and the temperature, respectively. For a chain of N tunnel junctions we have previously shown[8] that the free-energy is given by the sum of the energy stored on each capacitor and the leads

$$G(\mathbf{n}) = \frac{1}{2}\sum_{i=1}^{N-1} C_{g,i}(\phi_i - V_{g,i})^2 + \frac{1}{2}\sum_{i=1}^{N} C_i(\phi_i - \phi_{i-1})^2 - V_e Q_e - V_c Q_c - \sum_{i=1}^{N-1} V_{g,i} Q_{g,i} + \frac{1}{2}\sum_{i=1}^{N-1} C_{s,i}\phi_i^2. \tag{2}$$

The potential on each of the islands is represented by the vector $\boldsymbol{\phi} \equiv (\phi_1, \phi_2, \ldots, \phi_{N-1})$, where ϕ_0 and ϕ_N represent the potentials of the leads, V_e and V_c. The charges on the left and right leads and the gate i are $Q_e = C_1(V_e - \phi_1) + en_e$, $Q_c = C_N(V_c - \phi_{N-1}) + en_c$, and $Q_{g,i} = C_{g,i}(V_{g,i} - \phi_i)$, respectively. The last term on the right-hand side of Eq. (2) represents the energy stored due to the self-capacitance of the island. After some algebra and elimination of the ϕ_i,[44] the free-energy difference can be expressed as

$$\begin{aligned}\Delta G_k(\mathbf{n}) = &-\frac{e^2}{2}(R_{k-1,k-1} + R_{k,k} - R_{k-1,k} - R_{k,k-1}) \\ &+ e\sum_{i=1}^{N-1} Q_i(R_{i,k-1} - R_{i,k}) + e(V_e - V_{g,1})A_{1,k} \\ &+ e\sum_{i=2}^{N-1}(V_{g,i-1} - V_{g,i})A_{i,k} + e(V_{g,N-1} \\ &- V_c)A_{N,k} - e\sum_{i=1}^{N-1} C_{s,i}V_{g,i}(R_{i,k-1} - R_{i,k}),\end{aligned} \tag{3}$$

where $A_{i,k} = C_i(R_{i-1,k} + R_{i,k-1} - R_{i-1,k-1} - R_{i,k}) + \delta_{i,k}$ and we define $R_{i,N} = R_{0,i} = 0$. Equation (3) gives the free-energy difference in terms of the external biases, charge occupancy, capacitances, and elements of the inverse capacitance matrix, $R_{i,j}$, and can be used to predict the threshold voltages for tunneling events to occur. Figure 5(a) shows numerical simulations of the tunneling rate and the solutions to $\Delta G_k(\mathbf{n}) = 0$ for the tunneling threshold voltages of a chain of six nanoparticles, each coupled to a common gate bias and with $V_c = 0$. The solid lines are obtained analytically by setting Eq. (3) equal to zero. The regions of dense contours correspond to increased conductance through the chain. The simulations and analytical results agree and predict that the conductance peaks will be equally spaced in voltage for all values of gate bias. In addition, differentiation of the simulated $I-V$ characteristics shows that the conductance peaks have approximately equal magnitude. In contrast, when the self-capacitance value is set to zero, the tunneling thresholds

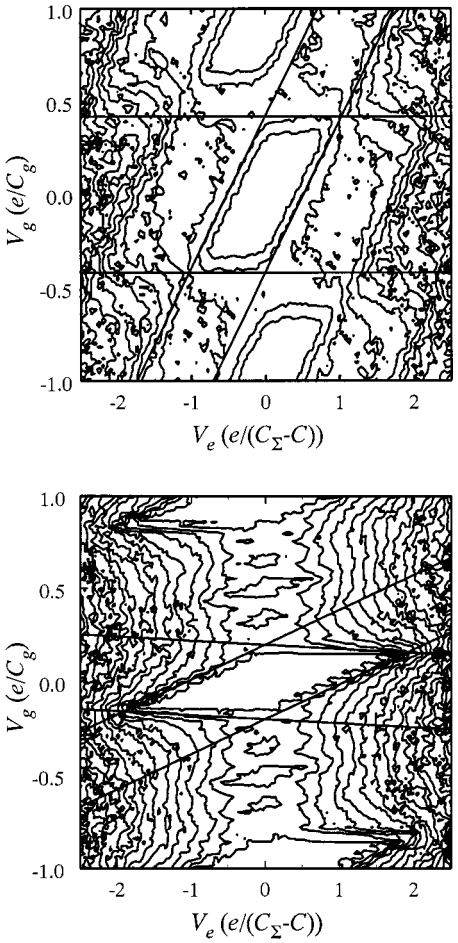

FIG. 5. (a) Plot of tunneling (contours) and the boundaries of the regions of stable electron occupancy (lines) of a chain of six nanoparticles as a function of gate bias and lead bias. (b) Plot of tunneling in which the self-capacitance has been set to zero.

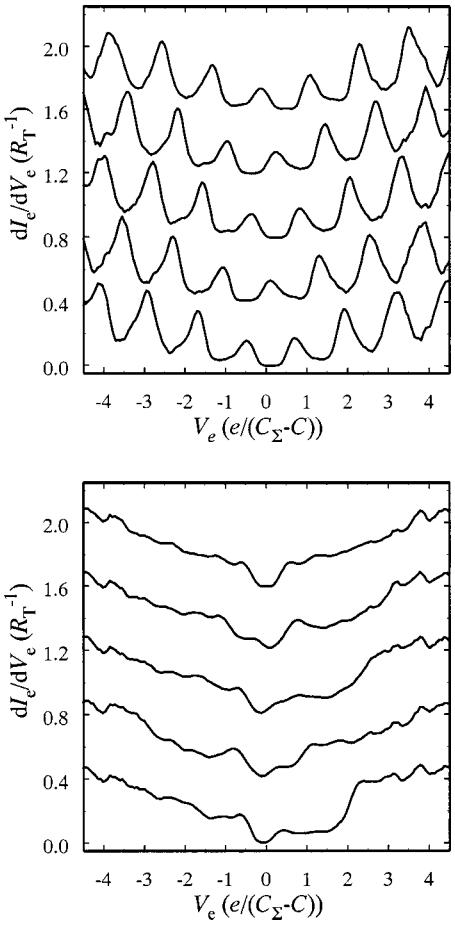

FIG. 6. Simulations of the differential conductance in units of inverse tunneling resistance of a six nanoparticle chain at random gate bias. Graph (a) shows the simulation results where the self-capacitance was included and graph (b) shows simulation results where the self-capacitance was neglected. Each simulation has been offset by an equal amount for clarity.

are very different; few distinctive conductance peaks are found and their separation is gate bias dependent, as shown in Fig. 5(b). We note that this regime is appropriate for traditional single electron devices, such as those based on Al/AlO tunnel junctions, where C_i and $C_{g,i}$ dominate over $C_{s,i}$.

To make a comparison between the model and the measured data, disorder in the samples must be taken into account. The types of disorder we have considered are variations in core size that influence $C_{s,i}$, the particle–particle spacing (positional disorder) that affect $C_{i,}$ the chain length and chain orientation.[24] Dispersion in C_i due to a distribution of particle–particle spacings was found to have little effect on the characteristics, which is not surprising for a system in which $C_{s,i} > C_i$. Numerical simulations of 756 randomly oriented chains were used to estimate the robustness of the periodic structure. Each chain had a different randomized set of capacitances with a distribution expected from the measured size distribution of the nanoparticles. Even with this degree of averaging, residual conductance periodicity was still found and the simulations provided a qualitative agreement to the $I-V$ characteristics.[24]

To replicate the effect of a time-varying background charge distribution, we used random values of the gate bias, V_g, in the numerical simulation and assumed that the same gate bias was coupled to each nanoparticle by an identical gate capacitor. The simulation results illustrated in Fig. 6 show the conductance peak behavior for chains where $C_{s,i}$ were included (a) and where they were set to zero (b). When the self-capacitance is included, Fig. 6(a), the effect of a gate bias on the $I-V$ characteristics is to shift the position of the conductance peaks along the nearly flat background without significantly changing the peak heights. In contrast, when the self-capacitance is ignored the simulations predict very different behavior as shown in Fig. 6(b). In this case, the conductance peak separations are not uniform nor are the peak heights constant. The striking resemblance between the measured changes in the conductance of the PLL-nanoparticle complexes (Fig. 3) and the simulations that include the self-capacitance [Fig. 6(a)] support the interpretation that the shifting conductance peaks are the result of a randomly fluctuating background charge. At this time we do not know the nature or origin of the background charge. Likely candidates include trapped charge in the substrate, charges trapped on individual nanoparticles that remain isolated on the surface after processing, charges trapped in defect states of the PLL, or ionized side chains of the PLL. The only observation we can make is that the time spent in a given charge state ap-

pears to be longer than a typical $I-V$ sweep time of about one hour.

IV. CONCLUSION

In summary, we have shown that the electrical properties of a collection of chains of nanoparticles are consistent with single electron charging effects. The electronic degree of freedom is found to be time-independent and indicative of one-dimensional transport. We have extended the orthodox model of single electron charging to include the self-capacitance of the nanoparticles, which because of geometry is the dominant capacitance. Simulations of the transport based on the modified model illustrate the importance of including self-capacitance, both for the static and temporal conductance. The results strongly suggest that the room temperature electrical behavior is sensitive to background charge fluctuations. The fact that such fluctuations can be detected points to the interesting possibility that nanoparticle-PLL assembles may be useful as highly sensitive chemical or biological sensors.[45]

ACKNOWLEDGMENTS

This work was supported in part by the Office of Naval Research, the National Science Foundation (DMR-9705343) and the Camille and Henry Dreyfus Foundation. J. E. Hutchison is an Alfred P. Sloan Research Fellow. Nippon Telephone and Telegraph Corporation generously donated the interdigitated electrodes with the 2 μm spacing. Lydia Longstreth was supported through the NSF–REU program (DMR-9820408).

[1] C. J. Gorter, Physica (Amsterdam) **17**, 777 (1951).
[2] E. Darmois, J. Phys. Radium **17**, 210 (1956).
[3] I. Giaever and H. R. Zellor, Phys. Rev. Lett. **33**, 74 (1962).
[4] J. Lamb and R. C. Jaklevic, Phys. Rev. Lett. **20**, 1504 (1968).
[5] D. V. Averin and K. K. Likharev, J. Low Temp. Phys. **62**, 345 (1986).
[6] E. Ben-Jacob, D. J. Bergman, B. J. Matkowsky, and Z. Schuss, Phys. Rev. B **34**, 1572 (1986).
[7] M. Stopa, Phys. Rev. B **64**, 193315 (2001).
[8] C. A. Berven and M. N. Wybourne, Appl. Phys. Lett. **78**, 3893 (2001).
[9] G. Schmid, Inorg. Synth. **27**, 214 (1990).
[10] C. B. Murray, D. J. Norris, and M. G. Bawendii, J. Am. Chem. Soc. **115**, 8706 (1993).
[11] M. Brust, M. Walker, D. Bethell, D. J. Schiffrin, and A. Whyman, J. Chem. Soc. Chem. Commun. **7**, 801 (1994).
[12] T. G. Schaaff, G. Knight, M. N. Shafigullin, R. F. Borkman, and R. L. Whetten, J. Phys. Chem. B **102**, 10643 (1998).
[13] X. M. Lin, C. M. Sorensen, and K. J. Klabunde, J. Nanopart. Res. **2**, 157 (2000).
[14] L. O. Brown and J. E. Hutchison, J. Am. Chem. Soc. **119**, 12384 (1997).
[15] E. Braun, Y. Eichen, U. Sivan, and G. Ben-Yoseph, Nature (London) **391**, 775 (1998).
[16] K. Kawasaki, M. Mochizuki, and K. Tsutsui, Jpn. J. Appl. Phys., Part 1 **38**, 418 (1999).
[17] B. A. Korgel, S. Fullam, S. Connolly, and D. Fitzmaurice, J. Phys. Chem. B **102**, 8379 (1998).
[18] X. M. Lin, R. Parthasarathy, and H. M. Jaeger, Appl. Phys. Lett. **78**, 1915 (2001).
[19] L. Clarke, M. N. Wybourne, M. Yan, X. S. Cai, and J. F. W. Keana, Appl. Phys. Lett. **71**, 617 (1997).
[20] R. P. Andres *et al.*, Science **272**, 1323 (1996).
[21] S. Datta, W. Tian, S. Hong, R. Reifenberger, J. I. Henderson, and C. P. Kubiak, Phys. Rev. Lett. **79**, 2530 (1997).
[22] D. L. Feldheim, K. C. Grabar, M. J. Natan, and T. E. Mallouk, J. Am. Chem. Soc. **118**, 7640 (1996).
[23] R. P. Andres, J. D. Bielefeld, J. I. Henderson, D. B. Janes, V. R. Kolagunta, C. P. Kubiak, W. J. Mahoney, and R. G. Osifchin, Science **273**, 1690 (1996).
[24] C. A. Berven, L. Clarke, J. L. Mooster, M. N. Wybourne, and J. E. Hutchison, Adv. Mater. **13**, 109 (2001).
[25] T. Sato, H. Ahmed, D. Brown, and B. F. G. Johnson, J. Appl. Phys. **82**, 696 (1997).
[26] S. H. M. Persson, L. Olofsson, and L. Gunnarsson, Appl. Phys. Lett. **74**, 2546 (1999).
[27] *Nanostructure Science and Technology, A Worldwide Study*, edited by R. W. Siegel, E. Hu, and M. C. Roco (Kluwer, Dordrecht, 1999).
[28] R. Parthasarathy, X. M. Lin, and H. M. Jaeger, Phys. Rev. Lett. **87**, 186807 (2001).
[29] N. Nishiguchi, Phys. Rev. B **65**, 035403 (2002); Jpn. J. Appl. Phys., Part 1 **40**, 1923 (2001).
[30] J. R. Heath, P. J. Kuekes, G. S. Snider, and R. S. Williams, Science **280**, 1716 (1998).
[31] C. P. Collier, E. W. Wong, M. Belohradský, F. M. Raymo, J. F. Stoddart, P. J. Kuekes, R. S. Williams, and J. R. Heath, Science **285**, 391 (1999).
[32] A. B. Zorin, F. J. Ahlers, J. Niemeyer, T. Weimann, H. Wolf, V. A. Krupenin, and S. V. Lotkhov, Phys. Rev. B **53**, 13682 (1996).
[33] N. M. Zimmerman, J. L. Cobb, and A. F. Clark, Phys. Rev. B **56**, 7675 (1997).
[34] M. Kenyon, J. L. Cobb, A. Amar, D. Song, N. M. Zimmerman, C. J. Lobb, and F. C. Wellstood, IEEE Trans. Appl. Supercond. **9**, 4261 (1999).
[35] D. E. Grupp, T. Zhang, G. J. Dolan, and N. S. Wingreen, Phys. Rev. Lett. **87**, 186805 (2001).
[36] M. Kenyon, J. L. Cobb, A. Amar, D. Song, N. M. Zimmerman, C. J. Lobb, and F. C. Wellstood, J. Low Temp. Phys. **123**, 103 (2001).
[37] A. A. Middleton and N. S. Wingreen, Phys. Rev. Lett. **71**, 3198 (1993).
[38] G. Y. Hu and R. F. O'Connell, Phys. Rev. B **49**, 16773 (1994).
[39] J. Rimberg, T. R. Ho, and J. Clarke, Phys. Rev. Lett. **74**, 4714 (1995).
[40] L. Clarke, M. N. Wybourne, M. Yan, S. X. Cai, L. O. Brown, J. Hutchison, and J. F. W. Keana, J. Vac. Sci. Technol. B **15**, 2925 (1997).
[41] D. V. Averin and K. K. Likharev, in *Mesoscopic Phenomena in Solids*, edited by B. L. Altshuler, P. A. Lee, and R. A. Webb (North Holland, Amsterdam, 1991), p. 240.
[42] G. L. Ingold and Y. V. Nazarov, in *Single Charge Tunneling, Coulomb Blockade Phenomena in Nanostructures*, NATO ASI Series, Series B Vol. 294, edited by H. Grabert and M. H. Devoret (Plenum Press, New York 1992).
[43] The capacitance matrix was calculated using FastCap© MIT (1992). For nanoparticles away from the end of a chain we find $C_i \approx 0.04$ aF and $C_{s,i} \approx 0.17$ aF. As expected, the value of $C_{s,i}$ is slightly larger than the value calculated for an isolated metal sphere of radius a coated with a dielectric shell, $C_{s,i} \approx 4\pi\varepsilon\varepsilon_0 a/[1+(a/d)(\varepsilon-1)] = 0.14$ aF, where d is the total radius of the core plus ligand shell.
[44] The island potentials can be eliminated by inverting the matrix equation $\mathbf{C}\boldsymbol{\phi}=\mathbf{Q}'$, where the capacitance matrix elements are given by, $\mathbf{C}_{i,j} = \delta_{i,j}(C_i + C_{i+1} + C_{g,i} + C_{s,i}) - \delta_{i+1,j}C_j - \delta_{i,j+1}C_i$ and Q_i' is given by $Q_i' = Q_i + C_{g,i}V_{g,i} + \delta_{i,1}C_1V_e + \delta_{i,N-1}C_NV_c$. The total charge on island i is Q_i which is given by the condition $C_{g,i}(\phi_i - V_{g,i}) + C_i(\phi_i - \phi_{i-1}) - C_{i+1}(\phi_{i+1} - \phi_i) + C_{s,i}\phi_{s,i} = Q_i$ and $Q_i = +en_i + Q_{0,i}$ where $Q_{0,i}$ is the offset background charge which is in the range $(-e/2, e/2)$ and n_i is an integer.
[45] W. P. McConnell, J. P. Novak, L. C. Brousseau III, R. R. Fuierer, R. C. Tenent, and D. L. Feldheim, J. Phys. Chem. B **104**, 8925 (2000).